ELSEVIER

Journal of Non-Crystalline Solids 293–295 (2001) 348–356

JOURNAL OF NON-CRYSTALLINE SOLIDS

www.elsevier.com/locate/jnoncrysol

Rigidity transitions in binary Ge–Se glasses and the intermediate phase

P. Boolchand *, X. Feng [1], W.J. Bresser

Department of Electrical and Computer Engineering and Computer Science, University of Cincinnati, 820 Rhodes Hall, Mail Location 30, Cincinnati, OH 45221-0030, USA

Abstract

Raman scattering measurements, undertaken on bulk Ge_xSe_{1-x} glasses at $0 < x < 1/3$, show evidence of two rigidity transitions as monitored by compositional trends in corner-sharing (ν_{CS}) and edge-sharing (ν_{ES}) $Ge(Se_{1/2})_4$ mode frequencies. A second-order transition from a floppy to an unstressed rigid phase occurs near $x_c(1) = 0.20(1)$ where both $\nu_{CS}(x)$ and $\nu_{ES}(x)$ show a kink. A first-order transition from an unstressed rigid to a stressed rigid phase occurs near $x_c(2) = 0.26(1)$, where $\nu_{CS}^2(x)$ displays a step-like discontinuity between $x = 0.25$ and 0.26 and a power-law behavior at $x > x_c$ (2). In sharp contrast, earlier micro-Raman measurements that use at least three orders of magnitude larger photon flux to excite the scattering, showed only one rigidity transition near $x_c = 0.23$, the mid-point of the intermediate phase ($x_c(1) < x < x_c(2)$). Taken together, these results suggest that the intermediate phase, observed in the low-intensity Raman measurements, undergoes a light-induced melting to a random network in the micro-Raman measurements.

1. Introduction

In the early 1980s, a *floppy*-to-*rigid* transition [1,2] in network glasses was predicted to occur when the number of valence force constraints per atom exceeds 3. The prediction has stimulated profound experimental and theoretical interest in glass science [3], other areas of condensed matter science [4] and even computer science [5]. In the past few years, the nature of the transition has been refined [6] by numerical simulations using the standard model of a glass as a random network. The numerical simulations start with a base network possessing a co-ordination number (CN), $r = 4$, such as a diamond lattice or a 4096-atom computer generated amorphous Si network with periodic boundary conditions. Bonds are depleted at random to produce networks of lower $\bar{r}$ in the $2 < \bar{r} < 4$ range insuring that no onefold co-ordinated atoms are produced. A Kirkwood or Keating potential is used to describe the α- and β-forces between atoms. The number of floppy modes/atom, $f(\bar{r})$, is then calculated as a function of $\bar{r}$ by performing a normal mode analysis at each $\bar{r}$. The results show a linear decrease in $f(\bar{r})$ in the $2 < \bar{r} < 2.35$ range, followed by an exponential tail in the $2.35 < \bar{r} < 2.70$ range. The onset of the rigidity transition is then localized by the second derivative, $\delta^2 f/\delta\bar{r}^2$, that reveals a sharp peak at $\bar{r}_c = 2.375(3)$ for the case of a diamond lattice, and at $\bar{r}_c = 2.385(3)$ for the case of a-Si base network. These results are remarkably close (within 1%) to

* Corresponding author. Tel. +1-513 556 4758; fax: +1-513 556 7326.

E-mail address: pboolcha@ececs.us.edu (P. Boolchand).

[1] Present address: Texas Instruments Inc., Stafford, TX 77477, USA.

0022-3093/01/$ - see front matter
PII: S0022-3093(01)00867-5

the mean-field result of $\bar{r} = 2.40$ for the onset of rigidity in *random networks* estimated by constraint counting. Such numerical calculations have also shown that in the rigid region, the elastic constants [7,8] display a power-law as a function of $\bar{r}$, with a power p of 1.4–1.5.

The Ge_xSe_{1-x} glass system was the subject of a previous micro-Raman and T-modulated DSC measurement in which evidence [9] for a first-order rigidity transition near $x_c = 0.23$ or $\bar{r}_c = 2(1 + x_c) = 2.46(1)$ was reported. In these micro-Raman measurements, several 100 μW of the 647.1 nm radiation from a Kr^+-ion laser, focused to a spot size <5 μm, was used to excite the scattering. Because of the high photon flux used in these micro-Raman measurements, one could not rule out the presence of light-induced modification of the rigidity transition.

To check the idea, we have now performed Raman measurements on the same Ge_xSe_{1-x} glass system in the same back scattering geometry, but this time in a conventional macro-mode with a loosely focused beam (< 500 μm spot size) resulting in a photon flux reduction by at least three orders of magnitude in relation to our previous micro-Raman measurements. These low-intensity Raman results are now reported in this work, and reveal that rigidity onsets in *two steps*. The *first transition* at $x_c(1) = 0.20$, occurs between a floppy and an unstressed rigid phase, and it is found to be of second order. The *second transition* at $x_c(2) = 0.26$ occurs between an unstressed rigid and a stressed rigid phase, and it is found to be of first-order. These results have close parallels in the companion Si_xSe_{1-x} binary glasses. These new results on a pair of IV–VI glasses represent the first examples of an *intermediate phase* ($x_c(1) < x < x_c(2)$) that separates the *floppy phase* ($x < x_c(1)$) from the *rigid phase* ($x > x_c(2)$). The present low-intensity Raman results when compared to the earlier micro-Raman measurements show a coalescing of the two rigidity transitions (at $x_c(1)$ and $x_c(2)$) into one localized at the mid-point $(x_c(1) + x_c(2)/2)$. The observation constitutes direct evidence for *photomelting* of the self-organized state of the backbone into a random network. The consequences of the observation on the general subject of rigidity onset in glasses is briefly commented upon.

2. Experimental procedure

Synthesis of the bulk glass samples used in this work is described in [9]. Some of the samples used in the present work were the ones used in our previous study. To cover a larger range of Ge concentrations, we synthesized additional samples as well. The glass transition temperatures of the samples were measured using a model 2920 MDSC from TA Instruments. 3 mW of 647.1 nm radiation from a Kr^+-ion laser was loosely focused to a spot size of about 500 μm on a glass sample to excite the Raman scattering. The back scattered radiation was analyzed with a triple monochromator system, model T64000 from Instruments SA, using a CCD detector. Under these operating conditions, we established glass sample temperature from the stokes/antistokes scattering ratio and found it less than 30 °C. The Raman lineshapes were deconvoluted in terms of Gaussians using a software package called Labcalc.

3. Experimental results

3.1. T-modulated DSC results (MDSC)

MDSC provides a means to deconvolute the total heat flow rate ($\dot{H}_t$) near T_g into a reversing heat-flow rate ($\dot{H}_r$) component and a non-reversing heat-flow rate $\dot{H}_{nr}$ component. Fig. 1(a) provides a summary of the $T_g(x)$ results on the relaxed glasses taken at a 3 °C/min scan rate and 1 °C/100 s modulation rate from the reversing heat flow rate. The non-reversing heat-flow $\Delta H_{nr}(x)$ variation with Ge concentration x appears in Fig. 1(b). The typical error associated with a datum is twice the size of the data point. For comparison, we have also shown in Fig. 1(a), the T_g variation in the companion Si_xSe_{1-x} binary glass system. T_gs for both glass systems at first increase linearly in the $0 < x < 0.08$ composition range. In Ge_xSe_{1-x} glasses, the T_g variation at higher x ($x > 0.20$) becomes super-linear, and displays a threshold behavior at $x = 1/3$. On the other hand, in Si_xSe_{1-x} glasses, $T_g(x)$ continue to increase with x even at $x > 1/3$. We shall return to comment on these contrasting trends later.

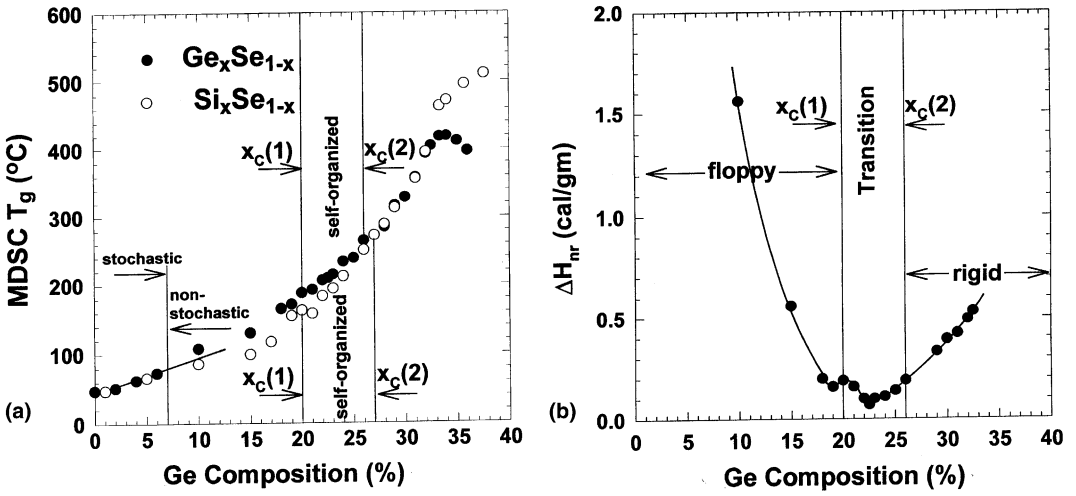

Fig. 1. (a) $T_g(x)$ variation in Ge_xSe_{1-x} and Si_xSe_{1-x} glasses deduced from the reversing heat flow in MDSC. See text for details. (b) Non-reversing heat-flow, $\Delta H_{nr}(x)$ variation in Ge_xSe_{1-x} glasses taken from [9]. The typical error associated with a datum is twice the size of the data point.

3.2. Raman scattering

Fig. 2 shows Raman spectra of the glasses obtained at selective compositions in the present work. The lineshapes show evolution of modes of corner-sharing (CS) tetrahedra (200 cm^{-1}) and edge-sharing (ES) $Ge(Se_{1/2})_4$ tetrahedra (215 cm^{-1}) at the expense of the Se–Se stretch mode of Se_n-chains (CM) at about 250 cm^{-1}. In general, CS and ES modes are symmetric and could be analyzed in terms of a Gaussian each. This was not the case for the CM, however, and it required at least two Gaussians for an adequate deconvolution at all x. Fig. 3 provides the mode frequency variation for each of the modes, from a comprehensive lineshape deconvolution of the Raman spectra.

Of particular interest are the CS and ES mode frequency ($\nu_{CS}(x)$ and $\nu_{ES}(x)$) variations shown in Figs. 3(a) and (b), respectively. In Fig. 3(a), one can discern a regime of a linear variation in $\nu(x)$ in the $0.08 < x < 0.20$ interval, and a regime of a power-law variation in the $0.26 < x < 1/3$ interval. In between these two regimes, lies a transition region ($0.21 \leqslant x \leqslant 0.25$) wherein the variation in $\nu(x)$ is sub-linear. To extract the underlying power-laws, we have made a plot of $\log_{10}(\nu_{CS}^2(x) - \nu_{CS}^2(0.26))$ against $\log_{10}(x - x_c(2))$, where $x_c = 0.26$,

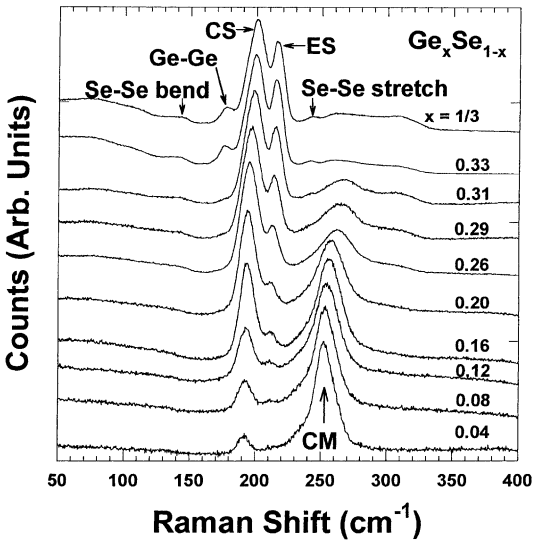

Fig. 2. Raman spectra of Ge_xSe_{1-x} glasses taken in a macro-mode, showing growth in scattering of corner-sharing mode (200 cm^{-1}) and edge-sharing mode (215 cm^{-1}) scattering of $Ge(Se_{1/2})_4$ units at the expense of Se_n -chain-mode scattering (250 cm^{-1}). See text for details.

and obtained the slope p_{CS} of the resulting line (Fig. 4(a)) and get a value of $p_{CS} = 1.54(6)$. A parallel analysis for the transition region (Fig. 4(b)) using $x_c(1) = 0.21$, yields a slope

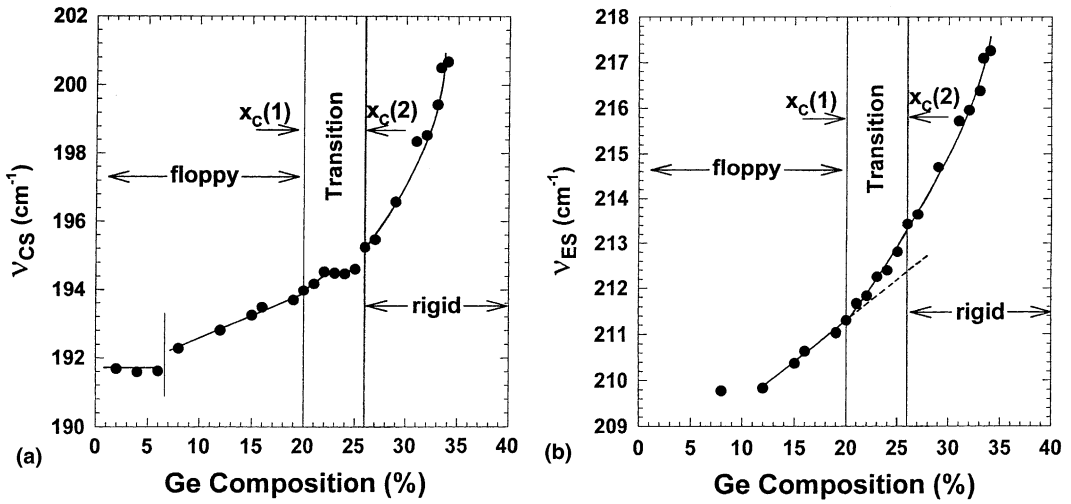

Fig. 3. Raman mode frequency variation of corner-sharing ($\nu_{CS}(x)$) and edge-sharing ($\nu_{ES}(x)$) tetrahedra plotted as a function of x in panels (a) and (b).

$p_t = 0.75(15)$. For the ES mode, our $\nu_{ES}(x)$ results suggest that the linear variation in $\nu(x)$ at low $x(0.10 < x < 0.20)$ smoothly connects to the power-law variation at higher x $(x > 0.21)$. Fig. 4(c) shows a plot of $\log_{10}(\nu^2_{ES}(x) - \nu^2_{ES}(0.21))$ against $\log_{10}(x - x_c(1))$ which yields a straight line with a slope $p_{ES} = 1.36(10)$, defining the underlying power-law associated with elasticity due to ES units.

Raman lineshape of Se_n-chains appears to be intrinsically asymmetric at all x, and analysis in terms of 1 Gaussian produced significant misfits, and required at least two Gaussians for a reasonable deconvolution. We have therefore analyzed this particular mode in terms of two Gaussians with minimal restrictions on lineshape parameters. One finds that the majority mode possesses a substantially broader linewidth than the minority mode. These trends for the CM in Ge–Se glasses are qualitatively similar to those of the CM reported [10] in the companion Si–Se glasses, though quantitative differences also exist. In sharp contrast to ES- and CS-mode frequencies, the CM frequency variation, $\nu_{CM}(x)$, provides no evidence of a power-law variation even in the rigid regime, as one would expect since these constitute the intrinsically floppy units of the network.

4. Discussion

4.1. Glass structure and $T_g(x)$ variation

Although the nature of the glass transitions continues to pose enormous challenges, considerable progress has been made in identifying the structure-related aspects of a network that influence the magnitude of T_g. The T_g of a network forming solid appears to be an intimate reflection of its *global connectivity*. Recently, the idea has been made rather quantitative, using the stochastic agglomeration theory [11,12]. The theory has provided a means to predict T_g as a function of glass composition. In particular, parameter-free predictions of $T_g(r)$ trends in binary, ternary and quaternary chalcogenides have been made using slope equations [12]. For a IV–VI glass system such as the present Ge_xSe_{1-x} binary, the slope equations predict

$$dT_g/dx = T_0/\ln r_{Ge}/r_{Se} = T_0/\ln 2. \quad (1)$$

Here T_0 is the glass transition of Se glass, and r_{Ge} and r_{Se} represent the co-ordination numbers (CNs) of Ge and Se of 4 and 2, respectively. In Fig. 1(a) the observed T_g trend at low x $(x < 0.08)$ for both binary glass systems closely match the slope

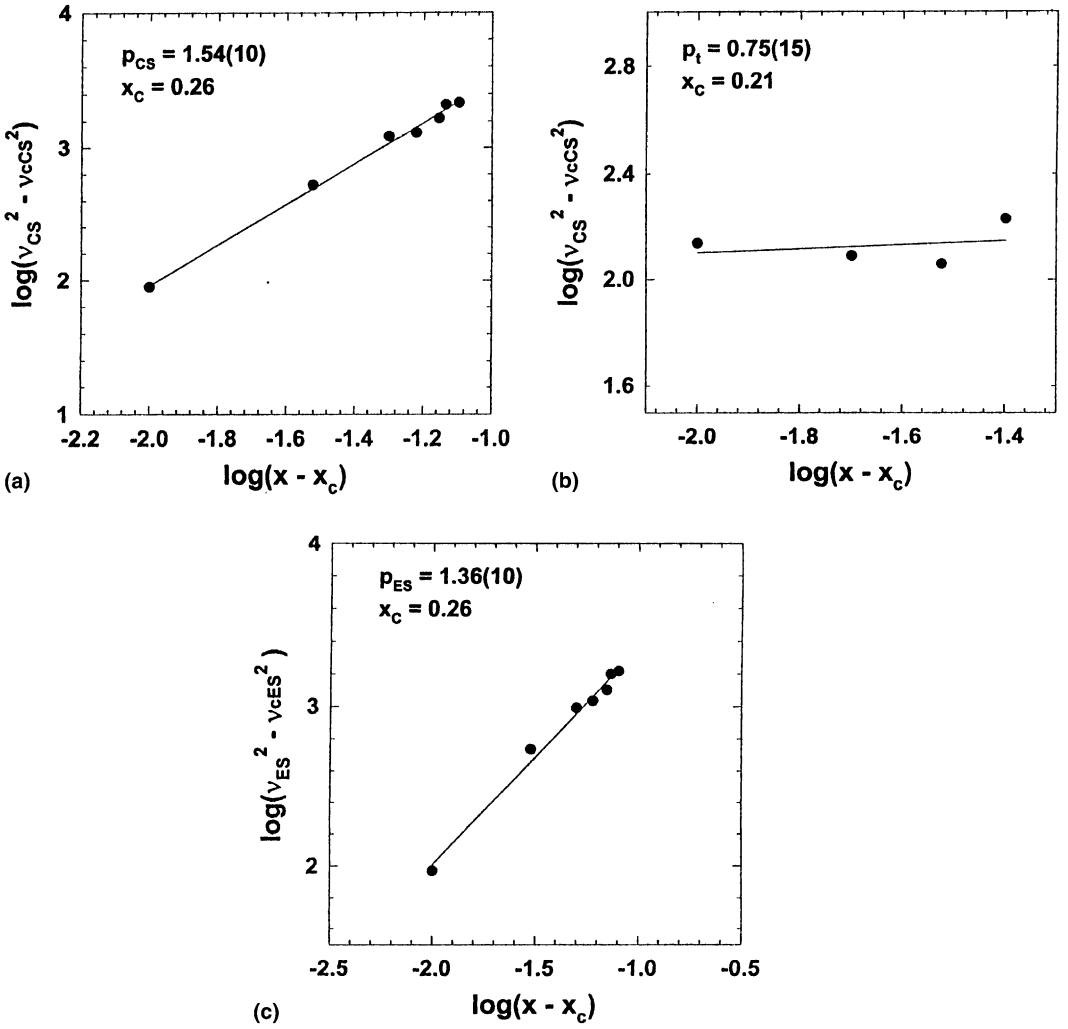

Fig. 4. Plots of $\log_{10}(v2 - v_C^2(x))$ against $\log_{10}(x - x_c)$ for CS mode frequency in panels (a) and (b) and ES mode frequency in panels (c). The plots give respective power-laws for CS mode based optical elasticity in the rigid region, p_{CS}, and transition region, p_t. The power-law variation of elasticity due to ES mode, p_{ES}, begins, on the other hand, at $x_c(1) = 0.21$ and appears in panel (c).

equation prediction (Eq. (1), straight line in Fig. 1(a)). These results suggest that a *stochastic* or *random network* description appears to be an appropriate one for these glasses at a low connectivity ($\bar{r} \leqslant 2.2$). At these low connectivities, $v_{CS}(x)$ and $\Gamma_{CS}(x)$ are largely independent of x or $\bar{r} = 2(1 + x)$.

At higher x ($x > 0.08$), the experimental T_gs become greater than the predicted T_gs (Eq. (1)). This suggests that select chemical configurations between CS tetrahedra and Se_n-chain fragments extending over 2 or 3 building blocks appear to be energetically preferred, thus lowering the global configurational entropy of the glass network. These results reflect the onset of a regime in which a *non-stochastic* structure evolves in these glasses as a precursor to the onset of rigidity at $x_c(1)$. It is precisely in this composition range ($0.15 < x < 0.25$) that the oversized Te tracer, in ^{129}I Mössbauer spectroscopy measurements [13], reveals a qualitative departure of site occupancies form a *stochastic variation*.

At still higher x ($x > 0.31$) a new feature of structure appears in the Ge–Se binary. Ge–Ge signatures first manifest [14] in Raman and Mössbauer spectroscopy measurements and continue to increase with x, leading to a small but reproducible concentration of homopolar bonds in the stoichiometric glass ($GeSe_2$) for which direct evidence from diffraction measurements [15] was recently provided. The maximum in T_g for the Ge–Se binary and the absence of such a threshold in the Si–Se binary suggests [14] that the Ge–Ge bonds do not form part of the backbone, while the Si–Si bonds in fact do when the latter first manifest at $x > 1/3$ in respective binary glass systems. These results are consistent with the notion that Ge–Se glasses at $x > 0.31$ may phase separate on a nanoscale, a point that is discussed elsewhere [14].

4.2. Non-reversing heat flow and network stress

In this section, we comment on a possible physical interpretation of the non-reversing heat flow term, ΔH_{nr}, before proceeding to discuss the central issue of this paper, viz., the rigidity transitions in the Ge_xSe_{1-x} glasses. The activation energies, $E_Y(x)$ for Kohlrausch relaxation of an *external stress* in ternary $Ge_xAs_xSe_{1-2x}$ glasses were reported (Fig. 5(b)) in flexural studies by Böhmer and Angell [16]. Recently, $\Delta H_{nr}(x)$ trends, in the same ternary glasses, have been measured (Fig. 5(a)) by Wang et al. [17]. These results reproduced in Fig. 5 show remarkably similar compositional trends, which consist of a global minimum of $\Delta H_{nr}(x)$ in the $2.28 < \bar{r} < 2.42$ range and an increase at both $\bar{r} > 2.42$ (rigid phase) and $\bar{r} < 2.28$ (floppy phase). An increase in both these observables in the rigid phase may be due to network stress buildup as rigid moities evolve in the backbone, and could be viewed as *enthalpic* in origin. Floppy modes proliferate at $\bar{r} < 2.28$, and their frequencies are finite, 5 meV or 40 cm^{-1} as revealed [18] by neutron vibrational density of states. The vanishing of the $\Delta H_{nr}(\bar{r})$ term in the $2.28 < \bar{r} < 2.42$ interval, constitutes evidence of the near absence of network stress in the backbone when the mean-constraints per atom equals 3 and the network becomes mechanically critical.

4.3. Rigidity transitions and self-organization

On general grounds one expects rigidity in the present glasses to nucleate at moities that include the overconstrained ($\bar{n}_c = 3.67$) building blocks such as the ES and CS units. In the Raman measurements, the scale of the mode frequencies ν_{CS}, ν_{ES} is set by the α- and β-force constants. However,

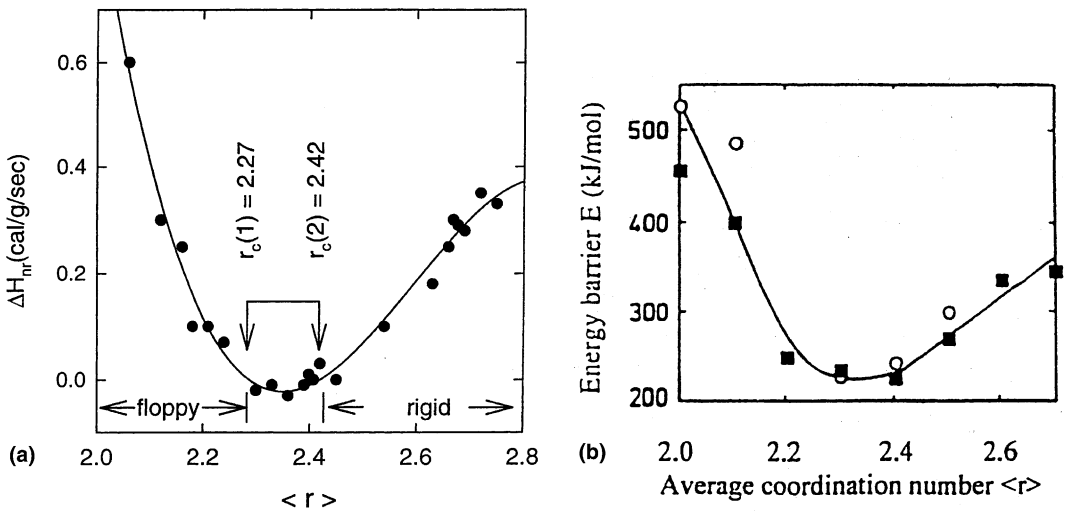

Fig. 5. (a) Non-reversing heat-flow variation, $\Delta H_{nr}(\bar{r})$ in $Ge_xAs_xSe_{1-2}x$ glasses, reported in [17]. (b) Activation energy for external stress relaxation in the same glasses, $E_Y(\bar{r})$ plotted as a function of $\bar{r}$ Bohmer and Angell. Both observables show remarkable parallel trends.

small increase in $v_{CS}(x)$ and $v_{ES}(x)$ with x as connectivity of the glasses increase, derives from the presence of intertetrahedral couplings. Such couplings would vanish only if the Se-bridging angles take on the special value of $\pi/2$. Ab initio molecular dynamic simulations [19] for the neutron structurefactor for $GeSe_2$ glass reveal that the Se-bridging angle displays a bimodal distribution centered at 100° and 80°. For these reasons, changes in v_{CS}^2 and v_{ES}^2 result from local or optical elasticities and can be expected to display a power-law variation with $\bar{r}$, once $\bar{r}$ exceeds a critical value $\bar{r}_c$ when the backbone becomes rigid, i.e.,

$$v^2 - v_C^2 = A(\bar{r} - \bar{r}_c)^p. \quad (2)$$

Numerical simulations [7,8] of random networks constrained by α- and β-forces show that the elasticity acquires a power-law variation given by Eq. (2) with a power $p = 1.4$.

The power-law variation of v_C^2 (Fig. 4(a)), starting at $x = x_c(2) = 0.26$ with $p_{CS} = 1.54(10)$, see Fig. 4, constitutes *direct evidence* for onset of *stressed rigidity*. The power-law $p_{CS} = 1.54$ is in excellent agreement with numerical estimates [7,8] of elasticity in random networks. Furthermore, the stressed nature of the backbone at $x > x_c(2)$ follows from the ΔH_{nr} heat-flow term which increases rapidly once $x > x_c(2)$ as illustrated in Fig. 1(b).

Our Raman experiments also show that rigidity first onsets at $x = x_c(1)$ in which both ES and CS units partake. This is suggested by the kink in $v_{CS}(x)$ and the onset of a power-law behavior in v_{ES}^2, both starting near $x_c(1)$. The optical elasticity associated with the rigid ES units yields a slightly lower power-law $p_{ES} = 1.36(10)$. We are less certain at present of the implications of this result. The composition $x_c(1)$ coincides with the lower bound of the global minimum in ΔH_{nr}, suggesting that in the $x_c(1) < x < x_c(2)$ interval glasses are largely unstressed. Furthermore, the transition at $x_c(1)$ appears to be second order as revealed by the continuous variation of mode frequencies $v_{CS}(x)$ and $v_{ES}(x)$.

The present experiments also suggest that at $x < x_c(1)$, glasses are floppy. Both $v_{CS}(x)$ and $v_{ES}(x)$ display a linear variation with x in the $0.10 < x < 0.20$ range with a small slope. In numerical simulations using the bond-depleted diamond lattice, elasticity in the floppy region vanishes. In these CNs simulations networks at different values of $\bar{r}$ are prepared by merely changing the concentration of C atoms possessing different CNs, of 2, 3 and 4. In the experiments, on the other hand, changes in $\bar{r}$ are brought about by alloying varying concentrations of Ge for Se, thus forming Ge–Se bonds at the expense of Se–Se bonds. Since the heteropolar bond possesses a higher chemical strength [20] than the homopolar one, one does expect elasticity of the network to increase due to strictly *chemical factors* rather than *topological ones*. It is for this reason the elasticity in the floppy region increases, even though the simulations predict a stationary value of zero.

Numerical simulations in self-organized networks were recently discussed by Thorpe et al. [21]. Building on their previous work, they noticed that once a network becomes rigid at a specific mean co-ordination number $\bar{r}_c^{\text{theory}}(\bar{r}_c^t) = 2.375$ (using the bond-depleted diamond lattice), they could self-organize the backbone by adding the additional cross-links at $\bar{r} > \bar{r}_c^t(1)$ *selectively* in the floppy regions of the network so as to drive them isostatically rigid, rather than to place them *randomly* and also drive some of the rigid regions to a stressed rigid state due to redundant bonds. The process of self-organization could only be continued up to an upper limit of $\bar{r}_c^t(2) = 2.392$ at which point the network makes a first-order transition to a stressed rigid state. The two transitions ($\bar{r}_c^t(1)$, $\bar{r}_c^t(2)$) in the simulations are strikingly parallel to the two ($\bar{r}_c(1)$, $\bar{r}_c(2)$) rigidity transitions observed in the present $Ge_x Se_{1-x}$ glasses. Also even through the absolute values of $\bar{r}_c^t(1)$ and $\bar{r}_c^t(2)$ obtained in these simulations depart from the observed thresholds quantitatively, the character of the predicted transitions match those observed in the experiments. One is therefore led to conclude that glasses in the $\bar{r}_c(1) < \bar{r}_c < r_c(2)$ interval are not only *stress-free* but also in a *self-organized state*.

4.4. Light-induced melting of the self-organized state in Ge_xSe_{1-x} glasses

To facilitate a comparison, we have reproduced the $v_{CS}(x)$ variation in Ge_xSe_{1-x} glasses from the

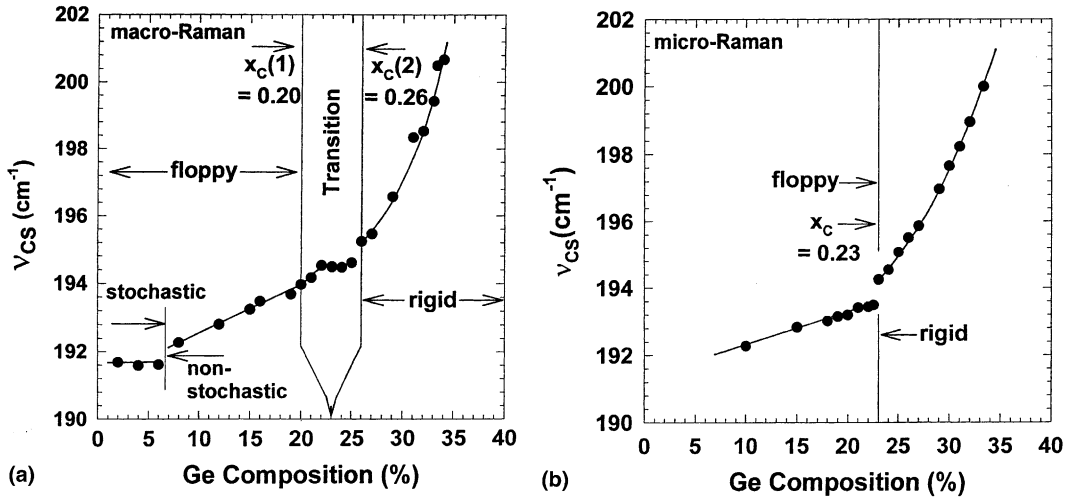

Fig. 6. Corner-sharing mode frequency variation, $\nu_{CS}(x)$, in Ge_xSe_{1-x} glasses from the present macro-Raman measurements (a) and from the earlier reported [9] micro-Raman measurements (b) compared. See text for details.

present *macro-Raman* (Fig. 6(a)) with the earlier *micro-Raman* (Fig. 6(b)) measurements. The photon flux in the micro-Raman measurements exceeds that in the present macro-Raman by at least four-orders of magnitude. One is therefore led to the suggestion that while the present *macro-Raman* investigations probe the *intrinsic* rigidity transitions of the glasses, the *micro-Raman* measurements probe a *light-induced modification* of these transitions. Certain features become transparent from the comparison of these results. The two transitions at $x_c(1) = 0.20$ and $x_c(2) = 0.26$ coelesce to a point at the centroid $x_c = (x_c(1) + x_c(2))/2 = 0.23$ location in the micro-Raman measurements. Furthermore, the centroid location $x_c = 0.23$ coincides with the global minimum in ΔH_{nr} heat flow term (Fig. 1(b)).

Our interpretation of these Raman and MDSC results is that the collapse of the intermediate phase to a solitary point in connectivity space is a photostructural effect. The high flux of near band gap radiation ($E_{photon} = 1.91$ eV) leads to a photomelting of the self-organized state to a random network. The underlying physical process probably consists of a transient self-trapped exciton that recombines non-radiatively leading to a light-induced dynamic state in which rapid bond-switching and diffusion occurs [22]. The photodiffusion process, apparently is optimized when the network stress vanishes and photomelting is the result. It is for this reason that the photomelted state is easily formed at the global minimum of the ΔH_{nr} term ($x_c = 0.23$), when network stress vanishes.

Parallel physical effects have recently been observed in Brillouin scattering measurements [23] on Ge–Se glasses. In these experiments, one found the longitudinal acoustic (LA) mode to soften qualitatively as a function of laser excitation power, but only for glass compositions in the center of the intermediate phase.

The Raman measurements on Ge_xSe_{1-x} glasses provide an essential link between the two extremal descriptions of the rigidity transitions in glasses. One observes two transitions [20] when the backbone is intrinsically *self-organized* in the melt-quenched glasses. One observes a solitary rigidity transition [7,8] characteristic of a *random network* in the photomelted state. And one expects that solitary transition to occur in connectivity space when $\bar{n}_c = 3$, as predicted by Phillips [1] and Thorpe [2] when they first proposed the idea.

5. Conclusions

Macro-Raman measurements on Ge_xSe_{1-x} glasses provide evidence of two rigidity transitions at $x_c(1) = 0.20$ and at $x_c(2) = 0.26$. The transition

at $x_c(1)$ is of a second order in optical elasticity and connects the floppy phase with the unstressed rigid phase. The transition at $x_c(2)$ is of first order in optical elasticity and connects the unstressed rigid to the stressed rigid phase. These elastic thresholds coincide with the non-reversing heat-flow, ΔH_{nr}, in T-modulated DSC measurements, which almost vanishes in the $x_c(1) < x < x_c(2)$ composition range. These rigidity transitions represent the lower ($x_c(1)$) and upper ($x_c(2)$) bounds of an intermediate phase that separates the floppy from the stressed rigid phase. The rigidity transitions coalesce at the centerpoint $[x_c(1) + x_c(2)]1/2 = 0.23$ when the exciting radiation flux for Raman scattering is increased by a few orders of magnitude. The collapse represents a photo-melting of the intermediate phase to a point in connectivity space when a random network is formed. The glass compositions corresponding to the photomelted state ($x_c = 0.23$) displays the smallest non-reversing heat-flow term in MDSC measurements. These results show that photo-melting of Ge_xSe_{1-x} glasses is facile when network stress vanishes.

Acknowledgements

It is a pleasure to acknowledge discussions with J.C. Phillips, M.F. Thorpe and R. Sooryakumar during the course of this work. This work is supported by grant DMR 97-01289 from US National Science Foundation.

References

[1] J.C. Phillips, J. Non-Cryst. Solids 34 (1979) 153; (For a more recent view see) J.C. Phillips, in: M.F. Thorpe, P.M. Duxbury (Eds.), Rigidity Theory and Applications, Kluwer Academic/Plenum, New York, 1999, p. 55.
[2] M.F. Thorpe, J. Non-Cryst. Solids 57 (1983) 355.
[3] For a review of experimental work on the subject, see P. Boolchand, in: P. Boolchand (Ed.), Insulating and Semiconducting Glasses, World Scientific, Singapore, 2000, p. 369.
[4] J.C. Phillips, Solid State Commun. 109 (1999) 301; J.C. Phillips, Proc. Nat. Acad. Sci. 95 (1998) 7264.
[5] R. Monasson, R. Zecchina, S. Kirkpatrick, B. Selman, L. Troyansky, Nature 400 (1999) 133.
[6] M.F. Thorpe, D.J. Jacobs, B.R. Djordjevic, in: P. Boolchand, World Scientific, Singapore, 2000, p. 95.
[7] H. He, M.F. Thorpe, Phys. Rev. lett. 54 (1985) 2107.
[8] D.S. Franzblau, J. Tersoff, Phys. Rev. Lett. 68 (1992) 2172.
[9] X.W. Feng, W.J. Bresser, P. Boolchand, Phys. Rev. Lett. 78 (1997) 4422.
[10] D. Selvanathan, W.J. Bresser, P. Boolchand, Phys. Rev. B 61 (2000) 15061;
D. Selvanathan, W.J. Bresser, P. Boolchand, B. Goodman, Solid State Commun. 111 (1999) 619.
[11] R. Kerner, M. Micoulaut, J. Non-Cryst. Solids 176 (1994) 271.
[12] M. Micoulaut, G. Naumis, Europhys. Lett. 47 (1999) 568.
[13] W.J. Bresser, P. Boolchand, P. Suranyi, Phys. Rev. Lett. 56 (1986) 2493.
[14] P. Boolchand, W.J. Bresser, Philos. Mag. B 80 (2000) 1757.
[15] I. Petri, P.S. Salmon, H.E. Fischer, Phys. Rev. Lett. 84 (2000) 2413.
[16] R. Böhmer, C.A. Angell, Phys. Rev. B 45 (1992) 10091.
[17] Y. Wang, P. Boolchand, M. Micoulaut, Europhys. Lett. 52 (2000) 633.
[18] W.A. Kamitakahara, R.L. Cappelletti, P. Boolchand, F. Gompf, D.A. Neumann, H.D. Mukta, Phys. Rev. B 44 (1991) 94.
[19] M. Cobb, D. Drabold, Phys. Rev. B 56 (1997) 3054.
[20] L. Pauling, in: Nature of the Chemical Bond, Cornell University, Ithaca, NY, 1960, p. 85.
[21] M.F. Thorpe, D.J. Jacobs, M.V. Chubynsky, J.C. Phillips, J. Non-Cryst. Solids 266–269 (2000) 859.
[22] For a recent review of light induced structural changes in glasses H. Fritzsche, in: P. Boolchand (Ed.), Insulating and Semiconducting Glasses, World Scientific, Singapore, 2000, p. 653, and references therein.
[23] H. Xia, J. Gump, I. Finkler, R. Sooryakumar, W.J. Bresser, P. Boolchand (unpublished).